

Simulation of correlated diffusion of Si and B in thermally grown SiO₂

Masashi Uematsu,^{a)} Hiroyuki Kageshima, and Yasuo Takahashi^{b)}
NTT Basic Research Laboratories, NTT Corporation, Atsugi 243-0198, Japan

Shigeto Fukatsu and Kohei M. Itoh
*Department of Applied Physics and Physico-Informatics and CREST-JST, Keio University,
 Yokohama 223-8522, Japan*

Kenji Shiraishi
Institute of Physics, University of Tsukuba, Tsukuba 305-8571, Japan

(Received 28 May 2004; accepted 23 August 2004)

Simultaneous diffusion of Si and B in thermally grown SiO₂ is modeled taking into account the effect of SiO molecules generated at the Si/SiO₂ interface and diffusing into SiO₂ to enhance both Si and B diffusion. Based on the model, we simulated experimental profiles of coimplanted ³⁰Si and B in ²⁸SiO₂, which showed increasing diffusivities with decreasing distance from the interface. The simulation results show that the SiO diffusion is so slow that the SiO concentration at the near-surface region critically depends on the distance from the interface. In addition, the simulation explains that the diffusivities of both Si and B increase with longer annealing times because more SiO molecules arrive from the interface. Furthermore, we examined the effect of high-concentration B on the diffusivities of Si and B in SiO₂, both of which increase with higher B concentration. The experimental results were simulated assuming that the diffusivity of SiO, which enhances the diffusivities of Si and B, increases with higher B concentration. The present results indicate that Si and B diffusion in SiO₂ are correlated via SiO molecules; namely, the enhancement of SiO diffusion at high B concentrations also causes enhanced diffusion of both Si and B. © 2004 American Institute of Physics. [DOI: 10.1063/1.1806253]

I. INTRODUCTION

With the scaling down of metal-oxide-semiconductor (MOS) devices, an ultrathin SiO₂ layer is demanded for the gate oxide film of MOS devices. As the thickness of the SiO₂ layer decreases, atomic and molecular diffusion in SiO₂ becomes a fundamental issue. Concerning the diffusion of impurities, boron B penetration from the gate electrode through the thin SiO₂ layer into the Si substrate has been recognized as a serious problem.¹ This problem is also serious in high- κ gate dielectrics because an interfacial SiO₂ layer may form between high- κ gate films and Si substrates during postannealing.² With respect to the B penetration, B diffusion in SiO₂ has been studied experimentally and theoretically.³⁻⁸ For Si self-diffusion, we have found, based on experimental and simulation results that SiO molecules generated at the Si/SiO₂ interface and diffusing into SiO₂ enhance Si self-diffusion in SiO₂.^{9,10} This suggests that the effect of the Si/SiO₂ interface must be taken into account in thermal processing involving ultrathin SiO₂ layers.

Recently, we have simultaneously observed Si self-diffusion and B diffusion in ²⁸SiO₂ samples coimplanted with ³⁰Si and B.¹¹ Both Si self-diffusivity and B diffusivity increase with decreasing distance from the Si/SiO₂ interface, which indicates that the SiO molecules from the interface govern not only Si self-diffusion but also B diffusion. In addition, both Si self-diffusivity and B diffusivity increase as B concentration increases, indicating faster SiO diffusion

with higher B concentration in SiO₂. In the present work, we constructed a model in which SiO molecules generated at the interface and diffusing into SiO₂ enhance both Si self-diffusion and B diffusion in SiO₂. Based on the model and assuming faster SiO diffusion with higher B concentration, we simulated the diffusion profiles of coimplanted ³⁰Si and B in ²⁸SiO₂ for various temperatures, SiO₂ thicknesses, annealing times, and B concentrations by using the same single set of parameters. The results indicate a correlation between Si self-diffusion and B diffusion in SiO₂, and that the Si and B interact with SiO arriving from the Si/SiO₂ interface.

II. SIMULATION MODEL

A. Diffusion model

Diffusion profiles of Si and B in SiO₂ simulated in this study were measured in ²⁸SiO₂ samples coimplanted with ³⁰Si and B. The sample structure employed is shown in Fig. 1. Thermally grown ²⁸SiO₂ samples (thicknesses of 200, 300,

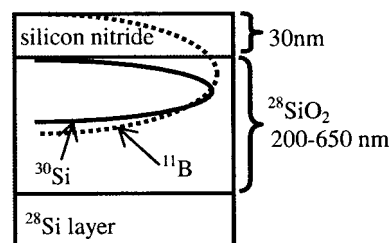


FIG. 1. The sample structure used for the experiments from which the diffusion profiles simulated in the present study were obtained.

^{a)}Electronic mail: uematsu@aecl.ntt.co.jp

^{b)}Present address: Hokkaido University, Sapporo 060-0814, Japan.

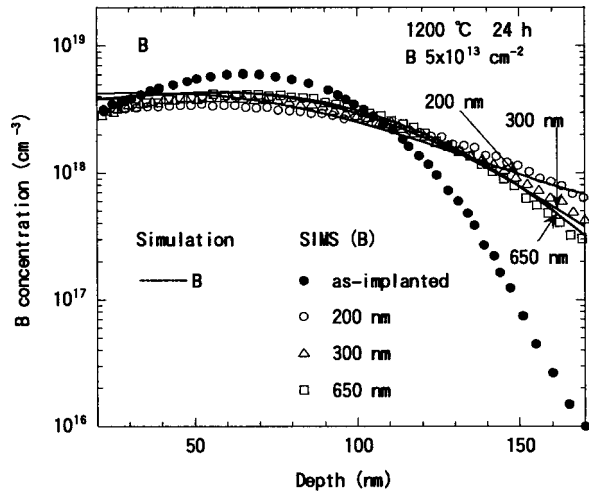


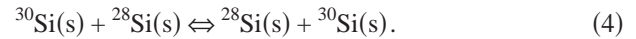
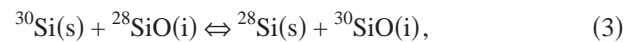
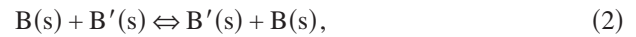
FIG. 2. Simulated and experimental B depth profiles in low-B-dose samples with various thicknesses after annealing at 1200 °C for 24 h. The as-implanted B profile is shown as the initial profile.

and 650 nm) were implanted with ^{30}Si at 50 keV to a dose of $2 \times 10^{15} \text{ cm}^{-2}$ and capped with a 30 nm thick silicon nitride layer. Subsequently, the samples were implanted with ^{11}B at 25 keV to a dose of $5 \times 10^{13} \text{ cm}^{-2}$ or $3 \times 10^{15} \text{ cm}^{-2}$, which are referred to as low-dose and high-dose samples, respectively. The implantation energy was chosen so that the peak position of implanted B would be close to that of ^{30}Si . Samples were preannealed at 1000 °C for 30 min to eliminate implantation damage and then diffusion annealed at 1100–1250 °C. We mention that there should be no concern that the implantation damage and strain in SiO_2 could play a role in the diffusion of Si and B because (i) the preannealing was performed prior to the diffusion anneals; (ii) the Si self-diffusivity remains unchanged for the ^{30}Si implantation doses between $1 \times 10^{14} \text{ cm}^{-2}$ and $2 \times 10^{15} \text{ cm}^{-2}$;⁹ (iii) the self-diffusivity of implanted Si in thick SiO_2 agrees with that obtained from damage-free chemical vapor deposition SiO_2 ;¹² and (iv) the Si self-diffusion, which increases with time due to increasing amounts of SiO arriving from the Si/ SiO_2 interface,¹⁰ would decrease with time if the diffusion were affected by the strain or damage, which should be gradually relieved or reduced by the anneals. The same time dependence was also observed for the B diffusion, as will be shown below.

First, we simulated the diffusion profiles with the low B dose to investigate the diffusion without the effect of high-concentration B. Figure 2 shows the experimental B depth profiles in low-dose samples with various thicknesses after annealing at 1200 °C for 24 h. The as-implanted profiles before preannealing are shown as initial profiles in the figures of this paper because the profiles after the preannealing showed no observable diffusion within the accuracy of our secondary-ion-mass spectroscopy (SIMS) measurements. The B profiles demonstrate a clear dependence on $^{28}\text{SiO}_2$ layer thickness; the thinner the $^{28}\text{SiO}_2$ layer is the higher the B diffusivity in SiO_2 . This tendency was observed consistently for other temperatures and annealing times employed in this study. This shows that the B diffusivity increases with decreasing distance from the Si/ SiO_2 interface, in the same

way as Si self-diffusion.^{9,10} The experimental signature of the B diffusivity enhancement with decreasing SiO_2 thickness is also found in Refs. 4 and 5, where highly B-doped poly-Si in MOS structures was used as the source of diffusing B.

The dependence of the distance from the interface on Si and B diffusion leads us to conclude that the SiO molecules, which are generated at the Si/ SiO_2 interface via the reaction $\text{Si} + \text{SiO}_2 \rightarrow 2\text{SiO}$ (Refs. 13 and 14) and diffusing into SiO_2 , enhance both Si self-diffusion and B diffusion. Consequently, we propose a model that the SiO molecules enhance both B and Si diffusion in SiO_2 via the reaction such that



In Eqs. (1) and (3), B and Si atoms substituted in the Si sites of SiO_2 [denoted as (s)] diffuse via the kick-out reaction with diffusing SiO molecules in interstitial sites [denoted as (i)]. In addition, a simple mechanism of B diffusion and Si self-diffusion via Si interstitials or vacancies is taken into account and is hereafter referred to as thermal B diffusion and Si self-diffusion. This mechanism is described by Eqs. (2) and (4), where SiO molecules are not involved in the diffusion. Evidence for the existence of two mechanisms (with and without SiO) is that very few SiO molecules arrive from the interface in the 650 nm thick sample, as will be shown below by the simulation results. B diffusion via SiO [Eq. (1)] is similar to B diffusion in Si via the kick-out mechanism, and B(i) may correspond to BO according to the first-principle calculation of B diffusion in SiO_2 .⁸

B. Diffusion equations

The above model leads to the following set of coupled partial differential equations to describe codiffusion of B and ^{30}Si in $^{28}\text{SiO}_2$:

$$\partial C_{\text{Bs}} / \partial t = \partial / \partial x (D_{\text{B(th)}}^{\text{eff}} \partial C_{\text{Bs}} / \partial x) - R_1, \quad (5)$$

$$\partial C_{\text{Bi}} / \partial t = \partial / \partial x (D_{\text{Bi}} \partial C_{\text{Bi}} / \partial x) + R_1, \quad (6)$$

$$\partial C_{^{30}\text{Si}} / \partial t = \partial / \partial x (D_{\text{Si(th)}}^{\text{SD}} \partial C_{^{30}\text{Si}} / \partial x) - R_2, \quad (7)$$

$$\partial C_{^{30}\text{SiO}} / \partial t = \partial / \partial x (D_{\text{SiO}} \partial C_{^{30}\text{SiO}} / \partial x) + R_2, \quad (8)$$

$$\partial C_{^{28}\text{SiO}} / \partial t = \partial / \partial x (D_{\text{SiO}} \partial C_{^{28}\text{SiO}} / \partial x) - R_1 - R_2, \quad (9)$$

where R_1 and R_2 are the reaction terms for Eqs. (1) and (3), respectively, described by

$$R_1 = k_{\text{f1}} C_{\text{Bs}} C_{^{28}\text{SiO}} - k_{\text{b1}} C_{\text{Bi}}, \quad (10)$$

$$R_2 = k_{f2}C_{30\text{Si}}C_{28\text{SiO}} - k_{b2}C_{30\text{SiO}} \quad (11)$$

The effective B diffusivity and the Si self-diffusivity are, as a whole, described by

$$D_B^{\text{eff}} = D_{B(\text{th})}^{\text{eff}} + D_i^{\text{eff}}C_{28\text{SiO}}(x,t)/C_{\text{SiO}}^0 \quad (12)$$

$$D_{\text{Si}}^{\text{SD}} = D_{\text{Si}(\text{th})}^{\text{SD}} + D_{\text{SiO}}^{\text{SD}}C_{28\text{SiO}}(x,t)/C_{\text{SiO}}^0 \quad (13)$$

In these equations, C_x is the concentration of the corresponding species in Eqs. (1)–(4), $D_{B(\text{th})}^{\text{eff}}$ the effective diffusivity of thermal B diffusion, $D_{\text{Si}(\text{th})}^{\text{SD}}$ the thermal Si self-diffusivity, D_{Bi} the diffusivity of B(i), D_{SiO} the diffusivity of SiO, and k_f and k_b are the forward and backward rate constants of Eqs. (1) and (3). In Eq. (12), $D_i^{\text{eff}} = D_{\text{Bi}}C_{\text{Bi}}^{\text{eq}}/C_{\text{Bs}}$ is the effective diffusivity of B diffusion via the kick-out mechanism with SiO, which corresponds to D_i^{eff} for B diffusion in Si.^{15,16} Here, $C_{\text{Bi}}^{\text{eq}}$ denotes the equilibrium concentration of B(i). In Eq. (13), $D_{\text{SiO}}^{\text{SD}} = D_{\text{SiO}}C_{\text{SiO}}^0/N_0$ is the self-diffusivity of Si via SiO molecules and the experimentally obtained $D_{\text{SiO}}^{\text{SD}} = 4.0 \times 10^4 \exp(-6.2 \text{ eV/kT}) \text{ cm}^2/\text{s}$ (Ref. 10) is used for the simulation. Here, N_0 denotes the number of SiO₂ molecules in a unit volume of silicon oxide, and C_{SiO}^0 denotes the maximum concentration of SiO interstitials in SiO₂ and is described as $C_{\text{SiO}}^0 = 3.6 \times 10^{24} \exp(-1.07 \text{ eV/kT}) \text{ cm}^{-3}$,¹⁰ which is estimated from the product of the interstitial segregation coefficient for the Si/SiO₂ interface¹⁷ and the equilibrium self-interstitial concentration in Si.¹⁸ In Eq. (5), the thermal B diffusion [Eq. (2)] is represented by the diffusion term with $D_{B(\text{th})}^{\text{eff}}$, and the experimentally obtained B diffusivity in thick SiO₂ ($>1 \mu\text{m}$) $D_{B(\text{th})}^{\text{eff}} = 3.12 \times 10^{-3} \exp(-3.93 \text{ eV/kT}) \text{ cm}^2/\text{s}$,⁶ which corresponds to the effective thermal B diffusivity is used in our simulation. In Eq. (7), the thermal Si self-diffusion [Eq. (4)] is represented by the diffusion term with $D_{\text{Si}(\text{th})}^{\text{SD}}$, and the experimentally obtained $D_{\text{Si}(\text{th})}^{\text{SD}} = 0.8 \exp(-5.2 \text{ eV/kT}) \text{ cm}^2/\text{s}$ (Ref. 12) is used for the simulation. In Eqs. (12) and (13), $C_{28\text{SiO}}(x,t)$ depends on the depth and annealing times, which has been described in Ref. 10. The boundary condition for ²⁸SiO(i) at the ²⁸Si/²⁸SiO₂ interface is given by $C_{28\text{SiO}}(x=\text{interface}) = C_{\text{SiO}}^0$ to describe the generation of SiO at the interface. The amount of ³⁰SiO(i) arriving at the ²⁸Si/²⁸SiO₂ interface is so small that the mixing of ²⁸Si with ³⁰Si at the interface is neglected. The boundary condition at the nitride-capped surface is represented by a zero-flux condition because the cappings act as barriers. Reactions (1)–(4) are assumed to be so fast that the local equilibrium of the reaction is established, and hence the rate constants are set to be large enough. In addition, Si and SiO₂ are thermodynamically in equilibrium with SiO with a certain solubility in SiO₂, which only depends on temperature. At the interface, SiO is therefore generated until this solubility value has been reached and a higher concentration of SiO leads to decomposition of SiO into Si and SiO₂. Interfacial reactions are generally much faster than one-dimensional diffusion away from an interface. Therefore, we assume that the generation rate of SiO at the interface is large enough so that the SiO concentration at the interface is fixed at C_{SiO}^0 . Consequently, the only parameter needed to fit the experimental ³⁰Si and B profiles is D_i^{eff} , and we consis-

TABLE I. Values of parameters used for the simulation.

Parameter	Value	References
$D_{\text{SiO}}^{\text{SD}}$	$4.0 \times 10^4 \exp(-6.2 \text{ eV/kT}) \text{ cm}^2/\text{s}$	10
$D_{\text{Si}(\text{th})}^{\text{SD}}$	$0.8 \exp(-5.2 \text{ eV/kT}) \text{ cm}^2/\text{s}$	12
D_i^{eff}	$6.4 \times 10^{-2} \exp(-4.1 \text{ eV/kT}) \text{ cm}^2/\text{s}$	Present work
$D_{B(\text{th})}^{\text{eff}}$	$3.12 \times 10^{-3} \exp(-3.93 \text{ eV/kT}) \text{ cm}^2/\text{s}$	6
C_{SiO}^0	$3.6 \times 10^{24} \exp(-1.07 \text{ eV/kT}) \text{ cm}^{-3}$	10

tently obtained $D_i^{\text{eff}} = 6.4 \times 10^{-2} \exp(-4.1 \text{ eV/kT}) \text{ cm}^2/\text{s}$ for all samples. Note that the calculated B profiles are fairly insensitive to the variation of the values of the individual parameters D_{Bi} and $C_{\text{Bi}}^{\text{eq}}$ once the value of D_i^{eff} is fixed, in the same way as for the simulation of B diffusion in Si.^{15,16} The parameters used for the simulation are listed in Table I and their values are shown in Fig. 3. Equations (5)–(9) were solved numerically by the partial differential equation solver ZOMBIE.¹⁹

C. B concentration dependence

Figure 2 compares the simulated and experimental B profiles for the low-dose samples after annealing at 1200 °C for 24 h. The simulation results fit the experimental B profiles for all thicknesses using the same parameter values. This is in contrast to the B diffusivity obtained by a simple fitting, or under the assumption of a constant diffusion coefficient for each profile, which increases with decreasing SiO₂ thickness: 2×10^{-16} , 1×10^{-16} , $7 \times 10^{-17} \text{ cm}^2/\text{s}$ for 200, 300, 650 nm, respectively (the contribution from $D_{B(\text{th})}^{\text{eff}}$ at 1200 °C is $7 \times 10^{-17} \text{ cm}^2/\text{s}$ for all thicknesses). In addition, the simulation results also fit the ³⁰Si and B profiles for all ²⁸SiO₂ thicknesses in low-B-dose samples for various temperatures using the same parameter values for each temperature.

As shown above, both B and Si diffusion in low-B-dose samples can be simulated using the same single set of parameters. However, the same simulation of B diffusion for

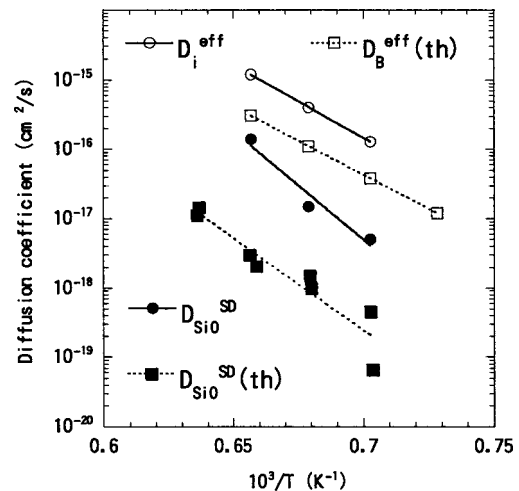


FIG. 3. Values of diffusivities used in the simulation. $D_{\text{Si}(\text{th})}^{\text{SD}}$ and $D_{B(\text{th})}^{\text{eff}}$ were experimentally obtained in Refs. 12 and 6, respectively, $D_{\text{SiO}}^{\text{SD}}$ was obtained from the simulation in Ref. 10, and D_i^{eff} was obtained to fit the experimental B and ³⁰Si profiles in the present study.

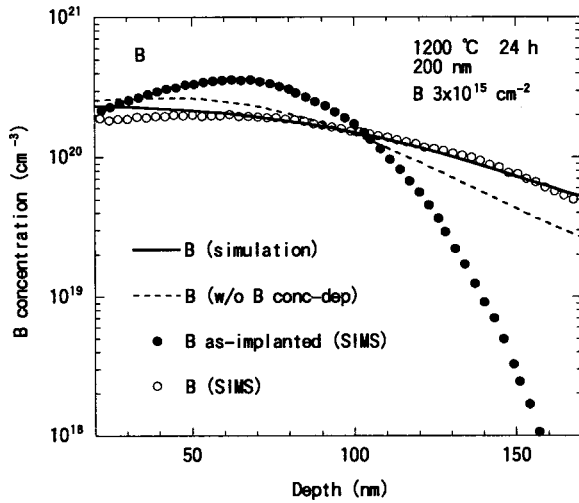


FIG. 4. Simulated and experimental B depth profiles in the 200 nm thick sample with high-B-dose after annealing of 24 h at 1200 °C. The result of simulation without B concentration dependence, which fits low-B-dose profiles, is also shown (dotted line).

high-dose samples underestimated the results, as shown by the dotted line in Fig. 4 for the 200 nm thick sample annealed at 1200 °C for 24 h. This result shows that B diffusion in high-dose samples is faster than that in low-dose samples. The B concentration dependence has been reported in an experiment using a MOS structure, where the B diffusivity abruptly increased above B concentration of 10^{20} cm^{-3} ,⁷ which is consistent with our result. In addition, we have found that Si self-diffusivity increases under a high B concentration in SiO_2 .¹¹ To reproduce the experimentally obtained enhancement of the Si and B diffusion in the high-dose sample, we introduced a B concentration dependence of $D_{\text{SiO}}^{\text{SD}}$, $D_{\text{Si}}^{\text{SD}}(\text{th})$, D_i^{eff} , and $D_B^{\text{eff}}(\text{th})$. These diffusivities are multiplied by a factor of $\exp(C_B/C_B^{\text{cri}})$ to imitate the strong dependence on B concentration, where C_B^{cri} denotes the critical B concentration above which the high-concentration effect occurs. In order to model the ^{30}Si and B diffusion via $^{28}\text{SiO}(\text{i})$ [Eqs. (1) and (3)], which are simultaneously enhanced by high-concentration B, $D_{\text{SiO}}^{\text{SD}}$ was multiplied by the factor $\exp(C_B/C_B^{\text{cri}})$. In addition, D_i^{eff} was multiplied by the same factor for the enhancement of B(i) diffusion because B atoms in SiO_2 diffuse with frequent atomic exchange interactions with SiO molecules, which diffuse predominantly through interstitial sites, according to the theoretical results.⁸ Furthermore, inclusion of the B concentration dependence [$\times \exp(C_B/C_B^{\text{cri}})$] of $D_{\text{Si}}^{\text{SD}}(\text{th})$ and $D_B^{\text{eff}}(\text{th})$ is essential for explaining the enhancement of ^{30}Si self-diffusion and B diffusion in the 650 nm thick sample, as described below. Consequently, the factor $\exp(C_B/C_B^{\text{cri}})$ was applied to D_B^{eff} [Eq. (12)] and $D_{\text{Si}}^{\text{SD}}$ [Eq. (13)], which represent the sum of the two contributions (thermal diffusion and diffusion via SiO) to B diffusion and Si self-diffusion, respectively. Using the value of $C_B^{\text{cri}} = 2 \times 10^{20} \text{ cm}^{-3}$, high-B-dose profiles were fitted by the same set of diffusion parameters as those for low-B-dose profiles, as shown in Fig. 4.

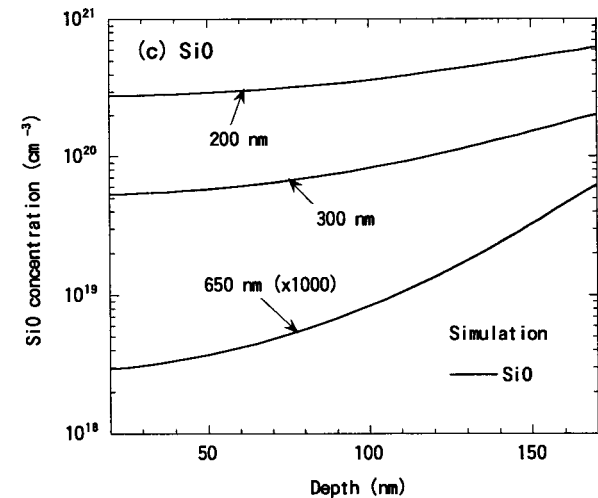
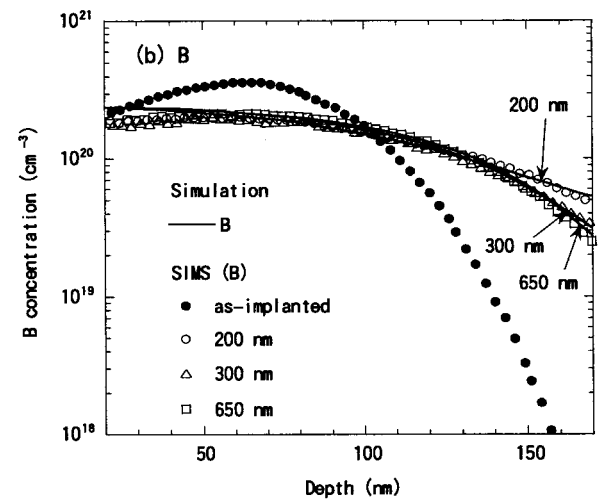
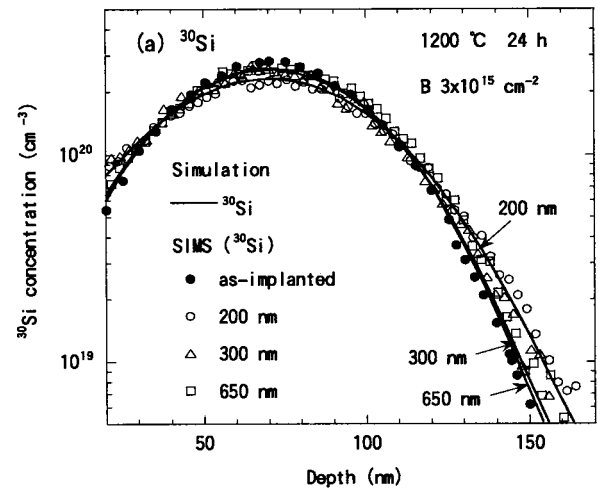


FIG. 5. Simulated and experimental (a) ^{30}Si and (b) B depth profiles and (c) simulated SiO profiles in high-B-dose samples with various thicknesses after annealing at 1200 °C for 24 h. The as-implanted ^{30}Si and B profiles are shown as the initial profiles.

III. RESULTS AND DISCUSSIONS

A. Distance dependence

Figure 5 shows the simulated and experimental ^{30}Si and B depth profiles in high-B-dose samples with various thicknesses after annealing at 1200 °C for 24 h together with the

simulated SiO profiles. For the simulated SiO profiles, the concentration of ^{28}SiO is shown because it is a few orders of magnitude larger than that of ^{30}SiO . In the same way as in low-B-dose samples, the Si self-diffusivity and B diffusivity, assuming constant diffusion coefficients, increase as the distance from the interface decreases in high-B-dose samples. The simulation results fit the experimental ^{30}Si profiles for all thicknesses using the same single set of parameters obtained from the low-dose B profiles described above. The profiles of SiO (that for the 650 nm thick sample is multiplied by 10^3) obtained from the simulation are shown in Fig. 5(c), and the SiO concentration in the ^{30}Si and B region increases with decreasing the $^{28}\text{SiO}_2$ thickness. The SiO concentration in the 650 nm thick sample is smaller than $1 \times 10^{17} \text{ cm}^{-3}$ in the depth region of this figure. This SiO concentration is so small that no enhancement of ^{30}Si and B diffusion via SiO occurs in the 650 nm thick sample. This means that the B diffusion and Si self-diffusion in the 650 nm thick sample take place almost totally via thermal diffusion [Eqs. (2) and (4)], not via the kick-out by SiO [Eqs. (1) and (3)]. This is the evidence for the existence of the two mechanisms (with and without SiO) and the reason for the inclusion of the B concentration dependence of $D_{\text{Si}}^{\text{SD}}(\text{th})$ and $D_B^{\text{eff}}(\text{th})$, which were described in Sec. II C. The SiO concentration in the ^{30}Si and B region increases with decreasing distance from the $^{28}\text{Si}/^{28}\text{SiO}_2$ interface. As expected from Eqs. (12) and (13), SiO with higher concentration leads to larger enhancement of B and ^{30}Si diffusion. Therefore, the B diffusivity and Si self-diffusivity, assuming constant diffusion coefficients, increase with decreasing $^{28}\text{SiO}_2$ thickness. This thickness dependence arises because the SiO diffusion is so slow that the SiO concentration at the ^{30}Si and B region critically depends on the distance from the Si/SiO₂ interface, where the SiO is generated. In Figs. 5(a) and 5(b), the diffusion of ^{30}Si and B in the 300 nm thick sample is only slightly larger than that in the 650 nm thick sample. As seen in Fig. 5(c), the SiO concentration in the 300 nm thick sample is not large enough to significantly enhance the ^{30}Si and B diffusion via SiO through the term $C_{\text{SiO}}/C_{\text{SiO}}^0$ in Eqs. (12) and (13), and the diffusion therefore mainly occurs through the thermal contributions $D_{\text{Si}}^{\text{SD}}(\text{th})$ and $D_B^{\text{eff}}(\text{th})$.

B. Time dependence

Figure 6 shows the simulated and experimental ^{30}Si and B profiles in the 200 nm thick sample with high-B-dose after annealing for 8 h and 24 h at 1200 °C together with the simulated SiO profiles. Both profiles were fitted by using the same single set of parameters used for the distance dependence. The simulated SiO concentration in the ^{30}Si and B region increases with increasing annealing time, as shown in Fig. 6(c). The Si self-diffusivities, assuming a constant diffusion coefficient, are $4 \times 10^{-18} \text{ cm}^2/\text{s}$ for 8 h and $1.6 \times 10^{-17} \text{ cm}^2/\text{s}$ for 24 h, and the B diffusivities are $1.5 \times 10^{-16} \text{ cm}^2/\text{s}$ for 8 h and $3.0 \times 10^{-16} \text{ cm}^2/\text{s}$ for 24 h. This time dependence arises because the SiO diffusion is so slow that the SiO concentration near the surface increases with annealing time until it reaches the maximum concentration

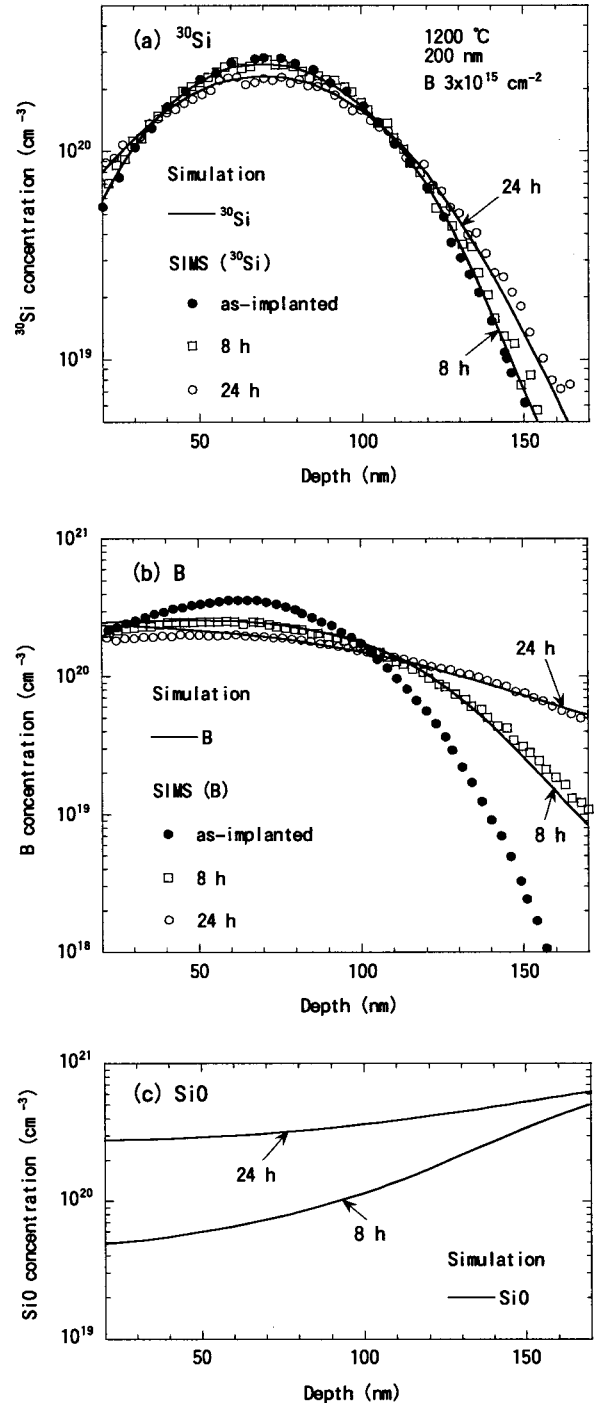


FIG. 6. Simulated and experimental (a) ^{30}Si and (b) B depth profiles and (c) simulated SiO profiles in the 200 nm thick sample with high B dose after annealing for 8 and 24 h at 1200 °C.

C_{SiO}^0 , and the Si and B diffusivities, assuming a constant diffusion coefficient, therefore increase for a longer annealing time. This time dependence leads to the ^{30}Si diffusion profile, which shows little diffusion after 8 h but a significant broadening after 24 h because the contribution of $D_{\text{Si}}^{\text{SD}}(\text{th})$ is so small (Fig. 3) that the total Si self-diffusion at 8 h becomes slow due to the small SiO concentration, leading to a small contribution of $D_{\text{SiO}}^{\text{SD}} C_{\text{SiO}}/C_{\text{SiO}}^0$ at 8 h. In contrast, the B diffusion profile at 8 h shows a significant broadening because the contribution of $D_B^{\text{eff}}(\text{th})$ is significant, as seen in Fig. 3.

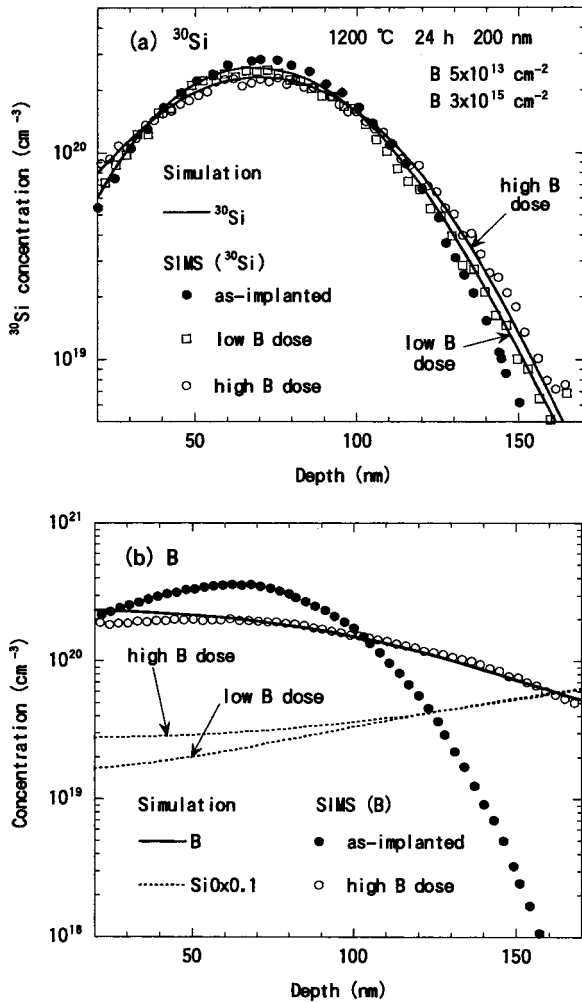


FIG. 7. Simulated and experimental (a) ^{30}Si and (b) B depth profiles and simulated SiO profiles (multiplied by 0.1) in the 200 nm thick sample with high- and low-B-doses after annealing for 24 h at $1200\text{ }^\circ\text{C}$. The B profile in the low-B-dose sample is shown in Fig. 2 (200 nm thick sample).

C. B concentration dependence

Figure 7 shows the simulated and experimental ^{30}Si and B profiles in the 200 nm thick sample with high and low B doses after annealing at $1200\text{ }^\circ\text{C}$ for 24 h together with the simulated SiO profiles multiplied by 0.1 (The B profile in the low-B-dose sample is shown by the 200 nm thick profile in Fig. 2). The experimental profile of ^{30}Si in the high-B-dose sample shows larger diffusion than that in low-B-dose samples. On the other hand, the ^{30}Si profile of the low-B-dose sample shows no significant difference from that without B. In addition, B diffusion in high-dose samples is faster than that in low-dose samples, as described in Sec. II C. The simulated results reproduce the experimental ^{30}Si and B profiles for both high-dose and low-dose samples using the same single set of parameters used for the simulation described above. The profiles of SiO for high and low B doses obtained from the simulation are shown in Fig. 7(b). In the near-surface region, the SiO concentration with high-B-dose is higher than that with low-B-dose, which leads to the increase of Si self-diffusivity and B diffusivity with higher B concentration.

Finally, we mention that the present results indicate that Si and B atoms in SiO_2 diffuse correlatively via SiO; namely, the enhanced SiO diffusion by the existence of high-concentration B enhances Si self-diffusion and B diffusion. This correlation is consistent with the theoretical result that SiO molecules diffuse predominantly through interstitial sites with frequent atomic exchange interactions with substitutional atoms.⁸ In addition, diffusion of SiO is closely related to the viscosity of SiO_2 .²⁰ Because viscosity is inversely proportional to diffusivity²¹ and the viscosity of SiO_2 strongly depends on the impurity content,²² the increase of SiO diffusivity may be closely related to decreasing SiO_2 viscosity with higher B doping.

IV. CONCLUSIONS

We have constructed a model in which SiO molecules generated at the interface and diffusing into SiO_2 enhance both Si self-diffusion and B diffusion in SiO_2 . Based on the model, we simulated and fitted the diffusion profiles of coimplanted ^{30}Si and B in $^{28}\text{SiO}_2$ for various temperatures, SiO_2 thicknesses, annealing times, and B concentrations by using the same single set of parameters. From the simulation, three characteristic features of the diffusion in SiO_2 were elucidated: (i) distance dependence from the Si/SiO₂ interface, (ii) time dependence, and (iii) B concentration dependence. The distance dependence arises because Si self-diffusion and B diffusion are enhanced as the SiO concentration at the ^{30}Si and B region increases with shorter distance from the interface. For the time dependence, the diffusivities of Si and B increase with longer annealing times because more SiO molecules arrive from the interface. The B concentration dependence of the diffusion indicates that the enhanced SiO diffusion by the existence of high-concentration B enhances both Si self-diffusion and B diffusion in SiO_2 and therefore Si and B atoms in SiO_2 diffuse correlatively via SiO.

ACKNOWLEDGMENTS

The authors thank U. Gösele and K. Yamada for fruitful discussions, H. Inokawa for B implantation, and A. Takano for SIMS measurements. The work was supported in part by a Grant-in-Aid for Scientific Research Nos. 14076215 and 14550020 and by "High-k Network" in cooperation with academic, industries, and governmental institutes.

- ¹J. R. Pfeister, L. C. Parrollo, and F. K. Baker, *IEEE Electron Device Lett.* **11**, 247 (1990).
- ²G. D. Wilk, R. M. Wallace, and J. M. Anthony, *J. Appl. Phys.* **89**, 5243 (2001).
- ³Y. Sato, K. Ehara, and K. Saito, *J. Electrochem. Soc.* **136**, 1777 (1989).
- ⁴R. B. Fair, *IEEE Electron Device Lett.* **17**, 242 (1996).
- ⁵R. B. Fair, *J. Electrochem. Soc.* **144**, 708 (1997).
- ⁶T. Aoyama, H. Tashiro, and K. Suzuki, *J. Electrochem. Soc.* **146**, 1879 (1999).
- ⁷T. Aoyama, H. Arimoto, and K. Horiuchi, *Jpn. J. Appl. Phys., Part 1* **40**, 2685 (2001).
- ⁸M. Otani, K. Shiraishi, and A. Oshiyama, *Phys. Rev. B* **68**, 184112 (2003).
- ⁹S. Fukatsu *et al.*, *Appl. Phys. Lett.* **83**, 3897 (2003).
- ¹⁰M. Uematsu, H. Kageshima, Y. Takahashi, S. Fukatsu, K. M. Itoh, K. Shiraishi, and U. Gösele, *Appl. Phys. Lett.* **84**, 876 (2004).
- ¹¹M. Uematsu, H. Kageshima, Y. Takahashi, S. Fukatsu, K. M. Itoh, and K. Shiraishi, *Appl. Phys. Lett.* **85**, 221 (2004).

- ¹²T. Takahashi, S. Fukatsu, K. M. Itoh, M. Uematsu, A. Fujiwara, H. Kageshima, Y. Takahashi, and K. Shiraishi, *J. Appl. Phys.* **93**, 3674 (2003).
- ¹³T. Y. Tan and U. Gösele, *Appl. Phys. Lett.* **40**, 616 (1982).
- ¹⁴G. K. Celler and L. E. Trimble, *Appl. Phys. Lett.* **54**, 1427 (1989).
- ¹⁵M. Uematsu, *J. Appl. Phys.* **82**, 2228 (1997).
- ¹⁶M. Uematsu, *Jpn. J. Appl. Phys., Part 2* **36**, L982 (1997).
- ¹⁷A. M. Agarwal and S. T. Dunham, *J. Appl. Phys.* **78**, 5313 (1995).
- ¹⁸H. Bracht, N. A. Stolwijk, and H. Mehrer, *Phys. Rev. B* **52**, 16542 (1995).
- ¹⁹W. Jüngling, P. Pichler, S. Selberherr, E. Guerrero, and H. W. Pötzl, *IEEE Trans. Electron Devices* **32**, 156 (1985).
- ²⁰R. H. Doremus, *J. Appl. Phys.* **92**, 7619 (2002).
- ²¹H. Eyring, *J. Chem. Phys.* **4**, 283 (1936).
- ²²A. J. Ikushima, T. Fujiwara, and K. Saito, *J. Appl. Phys.* **88**, 1201 (2000).